Journal of Petroleum Science and Technology 13(2): 38, 2023, Pages 40-45
DOI:10.22078/jpst.2023.5279.1908

Journal of Petroleum Science and Technology
Research Paper
https://jpst.ripi.ir/

Elemental Mercury Removal from Natural Gas by Cupper Sulfide Supported Alumina as a Sorbent

Ali Karimi[1]*, Sepehr Sadighi[1], Maryam Mashayekhi[1], Amir Zarei[2], Masoumeh Ghalbi Ahangary[2]
1-Catalysis Development Technologies Division, Research Institute of Petroleum Industry (RIPI), Tehran, Iran
2- Research Inistitute for the Development of Chemistry, Polymer and Petrochemical Technolog,, Research Institute of Petroleum Industry (RIPI), Tehran, Iran

Abstract
Feed streams of natural gas refineries and petrochemical industries contain mercury traces, threatening the environment and human health. Moreover, brazed aluminum heat exchangers are susceptible to being attacked by this component. The current research discusses the mercury removal capacities of alumina-based sorbents containing copper sulfide as an active metal. Cat-A and MRU-4 are synthesized and characterized using XRD, BET, TEM, XRF, and LECO methods. The experiments were carried out by loading the sorbents in a fixed-bed reactor, and they were sulfided by using a nitrogen gas stream containing 8 mol% of H_2S at the temperature of 285°C. Then, their mercury removal capacities are measured at the temperature of 60 °C, pressure of 1 atm, and gas flow rate of 220 cm^3/min versus time. Results showed that Cat-A and MRU-4 sorbents reached their static adsorption capacities of 12.1 and 19.3 wt%, respectively. Moreover, mercury adsorption variations of sorbents against time indicate that MRU-4 had faster dynamic adsorption than Cat-A sorbent. Ultimately, the characterization results also confirmed that the structures of MRU-4 and Cat-A adsorbents were mesoporous and microporous, respectively.

Keywords: Mercury Removal, Synthetic Gas, Activated Alumina, Copper Sulfide, Sorbent.

Introduction
Mercury contamination significantly damages human health and wildlife. Moreover, it can cause corrosion, contamination of equipment, catalyst poisoning, and toxicity through environmental emission [1-4]. Therefore, global initiatives have come into force to undertake drastic actions and raise public awareness against this element. Since the 1970s, cryogenic processing plants have faced the effect of mercury contamination, and consequently, numerous patents were published on abatement and remediation of mercury to solve this issue [5-7].

For gas-processing industries, some remedies for removing mercury have been proposed as purification solutions, in which regenerable and non-regenerable fixed-bed mercury removal methods are the favorites of industries. The latter method uses non-regenerative metal sulfide sorbents to eliminate mercury from the raw upstream of the dryer, amine unit, and especially the LNG process [7]. Various sorbents, such as activated carbon and selenium, are used for mercury adsorption, and their chemical modifications are carried out with sulfur, halogen, and noble metals [8-12].

Impregnating the surface of a support by using a metal sulfide is an effective method to enlarge mercury adsorption capacity, resulting from the fact that surface sulfur compounds provide sufficient binding sites for the formation of stable mercury sulfide (HgS) [12-13]. Metal sulfides act as proper adsorbents for eliminating mercury due to their extensive active sulfur sites, low cost, and environmental friendliness. Compared with some traditional sorbents, metal sulfides display excellent capability for eliminating mercury, and they are extremely resistant to H_2O and SO_2. To address this subject, nano-ZnS with a huge surface area was prepared which showed a superior mercury adsorption capacity to commercial activated carbons [14,15]. Moreover, it was proved that magnetic pyrrhotite as a recyclable sorbent was suitable to eliminate mercury from flue gas due to its excellent resistance to H_2O and SO_2 at low temperatures [16]. However, the mercury adsorption capacities of these metal sulfides were still too low to be used in real industrial applications. Therefore, developing metal sulfides supported on alumina sorbents with larger mercury adsorption capacity is still the key to controlling mercury emission. Copper sulfide supported on alumina provides abundant active sulfur sites for effectively eliminating mercury. In addition, literature indicated that Cu-terminated active sites have strong adsorption affinity for mercury [17].

**Corresponding author:* Ali Karimi, Catalysis Development Technologies Division, Research Institute of Petroleum Industry (RIPI), Tehran, Iran
E-mail addresses: karimialhasti@gmail.com
Received 2023-10-17, Received in revised form 2023-11-19, Accepted 2023-12-05, Available online 2024-02-12

In this research, adsorbents are synthesized by impregnating copper sulfide on alumina supports, and then their performances are evaluated for adsorbing mercury from natural gas. In this study, a synthetic gas (SG) is produced by evaporating the liquid mercury from a thermostat glass saturator into a stream of pure nitrogen. Then, the samples mercury adsorption capacities are calculated using a dynamic gravimetric method.

Materials and Methods

Sample Preparation and Characterization

S-A and S-4 supports are composed of gamma and activated alumina, respectively. S-A is a commercial activated alumina support, but S-4 is specifically synthesized in this research. To synthesize the latter, 12 g of commercial boehmite (Azarshahr, M2) was mixed with 0.32 g of HPMC (Hydroxypropyl methylcellulose, Sigma Aldrich, CAS 9004-65-3) and 0.2 g of Polyethylene glycol 6000 (Merck). Then, 21 ml of deionized water and 0.65 ml of HNO_3 (Merck, 65 wt%) were gradually added to the above mixture to form a homogenous paste. Extrudates (1.3 mm diameter and 5-8 mm length) obtained from this paste were dried at 120 °C for 2 h. Finally, extrudates were calcined at 550 °C for 4 h. For synthesizing sorbents, all supports were dried at 400 °C for 1 h, and cooled in a desiccator. After that, the $CuNO_3$ solutions were impregnated on them. Both sorbents were kept at the laboratory overnight and then dried in an oven till 120 °C for 2 h. Finally, they were calcined at 400 °C for 5 h. The produced sorbents should contain about 10 wt% of CuO, measured using XRF analysis.

The BET surface area, pore volume, and average pore radius of supports and sorbents were measured using an ASAP-2000 device from Micrometrics. Powder X-ray diffraction (XRD) measurements of sorbents were conducted using a Philips PW1840 X-ray diffractometer with monochromatized Cu/Ka radiation (λ = 1.5406 nm), and XRD patterns in the 2θ range of 0-90° were recorded [18-19]. The sorbents' sulfur contents were measured using a CS-125 carbon/sulfur analyzer. This method determines the total sulfur in petroleum products and other organic/inorganic materials using a LECO sulfur analyzer. Furthermore, the initial mercury concentration of the feed stream in experiments was measured with an ion SCIENCE MVI (Mercury Vapour Indicator) device.

Bench-scale Adsorption Tests

In Fig. 1, the schematic of the setup used for measuring the mercury adsorption capacity of samples is presented. SG is produced and fed into a fixed-bed reactor at the required temperature and the desired Hg concentration. This stream is created by evaporating the pure liquid mercury into a stream of pure nitrogen. The mercury saturator is made of a horizontal tube comprising seven empty glass spheres with an internal diameter (ID) of 30 mm conned by short and narrow glass tubes (ID and length of 1 and 4 mm, respectively). Each sphere is filled with 45 g of liquid mercury [20-21]. This design allows a relatively large gas-liquid contact area (in the sphere) and sufficient mixing between nitrogen and mercury vapor (in the tube). The existence of mercury is indicated by using an aqueous detector composed of $PdCl_2$ and CuI. The mass flow rate of pure nitrogen (N_2>99.9999%) is adjusted by using a mass flow controller (MFC), and its temperature is set at 60 °C by using a water circulation bath.

The diluted stream is fed to the fixed-bed reactor loaded with the sorbent to start the experiment. The ID and length of the reactor are 11 and 90 mm, respectively. This reactor is implemented inside a thermostat oven equipped with a temperature controller. The sorbents are crushed and meshed between 0.25 and 0.4 µm to increase the external film diffusion coefficient and internal mass transfer. It should be noted that small particle sizes increase the pressure drop along the fixed bed column and cause undesirable fluidization. Therefore, the bed is loaded with approximately 0.1 g of sorbent, and the sorbent is homogenously mixed with 7 g of crushed quartz beads in sizes between 595 and 841µm to avoid channeling. The experiments were conducted by sulfiding the loaded sample with nitrogen gas containing 8 mol% H_2S (Air Products, EINECS No.:2441658) at 285 °C for 12 h. The gas leaving the reactor passes through a solution containing 4 wt% of NaOH (commercial grade). After completing this step, the adsorption capacities of sorbents are evaluated at the temperature of 60 °C, pressure of 1 atm, and flow rate of 220 cm^3/min. The outlet of the reactor is passed through a solution containing 10 wt% of H_2SO_4 (Merck, 95-98%) and 4 wt% of $KMnO_4$ (Riedel CAS 31404). The experiments were repeated twice to confirm the reliability and repeatability.

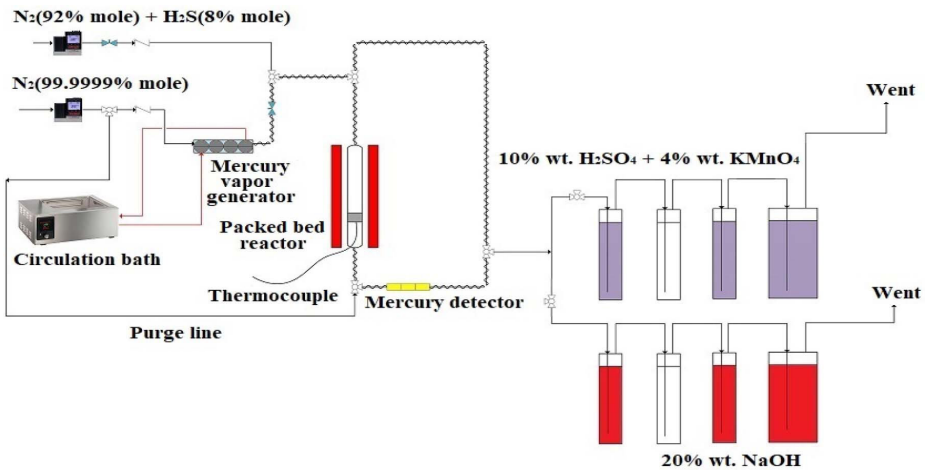

Fig 1. The schematic of the setup used for mercury removal studies.

Results and Discussion

BET surface area, pore volume, and average pore diameter of the synthesized and commercial supports are presented in Table 1. At first glance, S-A support with a BET surface area of 321 m^2/g seems superior to S-4. However, the pore volume of S-4 indicates that its support is more porous than S-A. The effects of the structural properties of these supports on the mercury removal capacity of sorbents will be discussed later.

Cat-A and MRU-4 are sorbent samples synthesized using S-A and S-4 supports, respectively. The characterization results of the synthesized sorbents are presented in Table 2. By comparing Tables 1 and 2, it is found that the impregnation process considerably reduces the surface area and pore volume of supports.

Cat-A and MRU-4 are sorbent samples synthesized using S-A and S-4 supports, respectively. The characterization results of the synthesized sorbents are presented in Table 2. By comparing Tables 1 and 2, it is found that the impregnation process considerably reduces the surface area and pore volume of supports.

As seen in Table 2, after impregnating and synthesizing sorbents, the reduction in the BET surface area of Cat-A with respect to its support is considerably higher than that of MRU-4 sorbent. Therefore, MRU-4 contains a greater number of mesopores in its structure than Cat-A, and the number of micropores of the latter is mostly occupied by the active metal. It is concluded that filling micropores of S-A by CuO significantly decreases the surface area of Cat-A sorbent.

Fig. 2 demonstrates the BET adsorption isotherm for Cat-A and MRU-4 sorbents. The IUPAC classification isotherm of Cat-A and MRU-4 are type II and type IV(a), respectively [22]. Based on this classification, Cat-A contains micropores, and MRU-4 is a mesoporous material containing pores 2-50 nm in width. This matter endorses our prediction about the pore size and placement of the active metal mentioned previously. Furthermore, XRF analyses confirm that all sorbents contain approximately 12 wt% of CuO with respect to the weight of their supports. Consequently, the metal contents of Cat-A and MRU-4 sorbents are equal; therefore, CuO content does not affect the mercury removal capacities of sorbents.

Fig. 3 shows XRD patterns of S-A and S-4 supports. According to the literature, the phase of S-A is activated alumina, and therefore, it exhibits a low degree of crystallinity. The maximum diffraction peaks and the main peak observed in its X-ray pattern are characteristic of γ-Al_2O_3. In contrast, the phase of S-4 (the support of MRU-4) is γ-Al_2O_3, with a high degree of crystallinity [23-24]. In this figure, standard references of gamma alumina couriers are observed at 2θ = 67.1°, 42.8°, 45.7°, 37.6° (JCPDS-00-01-1308) [25].

Table 1 The characteristic of supports used as sorbent samples.

Supports	Materials	BET surface area (m^2/g)	Pore volume (cm^3/g)	Average diameter (nm)
S-A	Activated alumina	321	0.37	4.60
S-4	Synthetic alumina	263	0.70	10.65

Table 2 The characteristics of sorbent samples.

Average diameter (nm)	Pore volume (cm^3/g)	BET surface Area (m^2/g)	Support	Sorbent samples
6.95	0.32	184	S-A	Cat-A
5.21	0.29	225	S-4	MRU-4

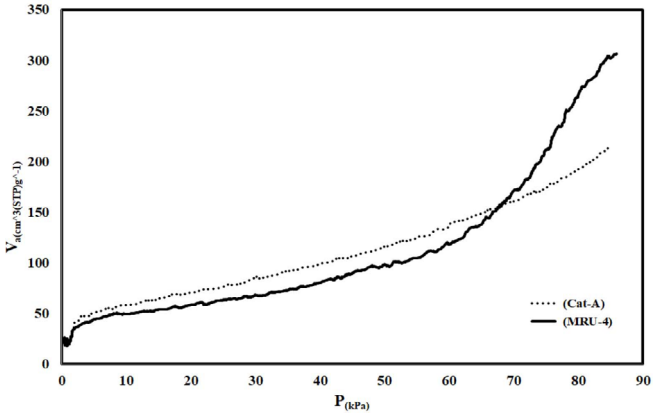

Fig. 2 BET adsorption isotherm for Cat-A and MRU-4 sorbents.

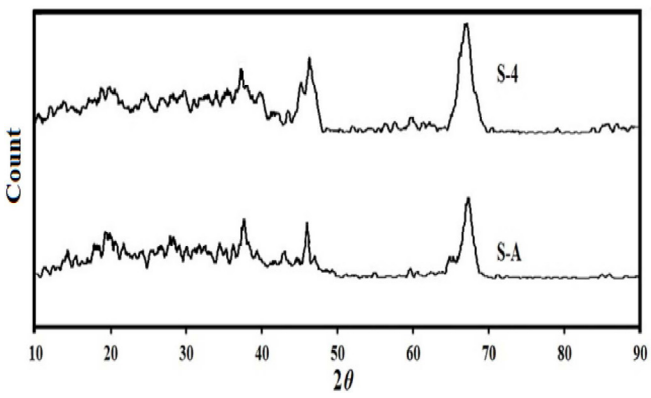

Fig. 3 XRD pattern for S-A and S-4 supports.

Moreover, Fig. 4 shows the XRD pattern of sulfided Cat-A and MRU-4 sorbents. The peaks at 2θ = 66.5 and 46.1 are related to alumina, and other peaks in the XRD pattern are associated with CuS pieces [19].

The TEM images of Cat-A and MRU-4 sorbents are presented in Fig. 5. Some black spots, which correspond to CuO particles, are detected in these images. The TEM image of MRU-4 sorbent demonstrates that particles are dispersed uniformly on the support, and its particles are smaller than that of Cat-A.

For measuring the mercury removal capacity after drying a sorbent, the weight loss is calculated at 300 °C. Moreover, oxygen atoms are converted to sulfur ones during the sulfidation of a sorbent, and the increase in its weight should be considered for calculating the mercury removal capacity. These data are obtained from analyzing sulfur content using the LECO device. After impregnating active metal on supports and synthesizing Cat-A and MRU-4 sorbents, mercury removal tests are dynamically carried out, and their outcomes are demonstrated in Fig. 6.

The results of the mercury removal tests after 330 min for Cat-A and MRU-4 sorbents are presented in Table 3. Accordingly, the mercury removal capacities of MRU-4 and Cat-A are 17.7 and 11.1 wt%, respectively.

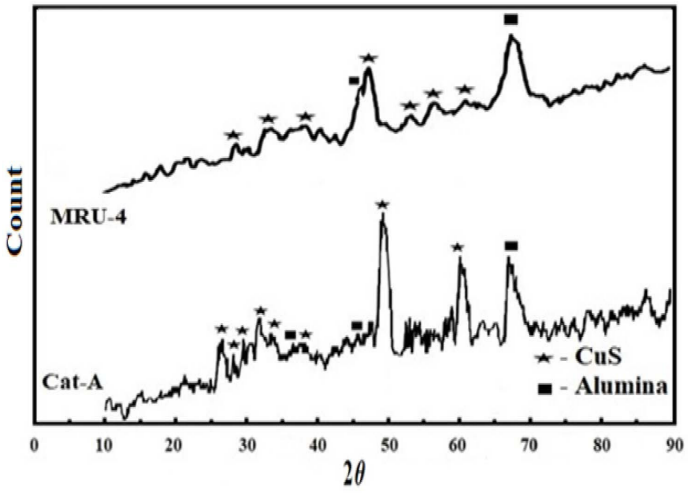

Fig. 4 XRD pattern for sulfided Cat-A and MRU-4 sorbents.

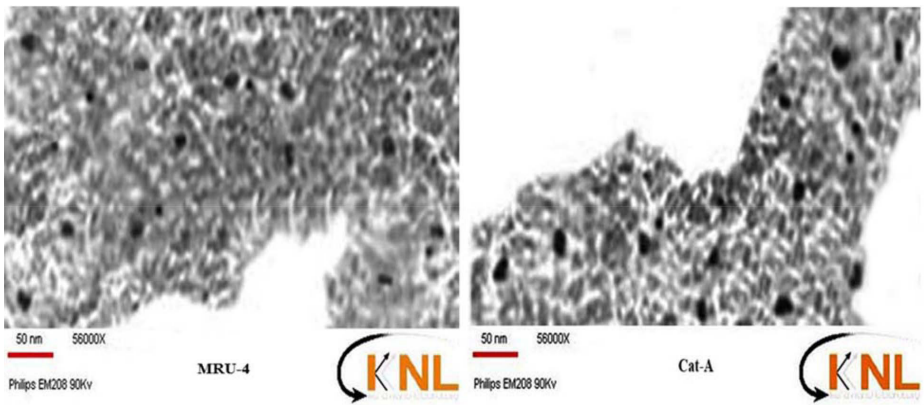

Fig. 5 TEM image of MRU-4 and Cat-A sorbents.

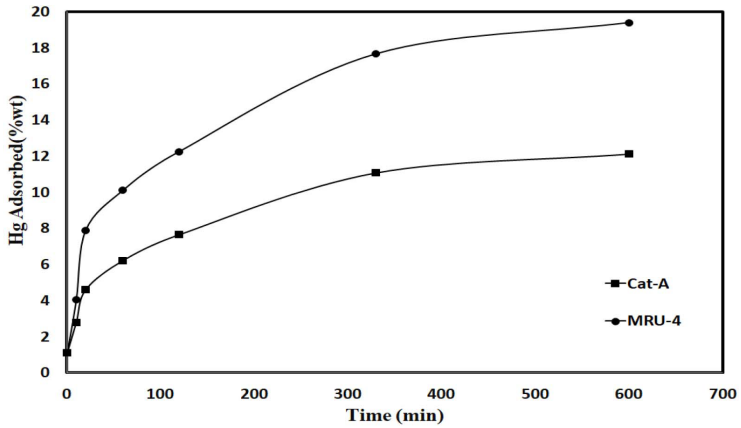

Fig 6 The capacity and breakthrough of mercury removal test of mercury removal sorbents.

Table 3 Calculation method for different sorbents in mercury removal test (time=330 min).

	Initial weight of sorbent (g)	Variation in the sorbent weight after heating @ 300 oC (g)	Variation in the sorbent weight after sulfidation (g)	Weight of sorbent after test (g)	Weight of mercury adsorbed (g)
Cat-A	0.1072	0.0990	0.0974	0.1092	0.0119
MRU-4	0.1111	0.1012	0.0991	0.1188	0.0197

Fig. 6 shows Cat-A and MRU-4 sorbents reach about 80% of their static adsorption capacities after about 330 minutes. After that, the Cat-A is almost saturated such that it can only adsorb about 1 wt% of mercury, while MRU-4 sorbent still has a 1.6 wt.% capacity to uptake. At 600 min, Cat-A and MRU-4 sorbents reach their static adsorption capacities of 12.1 and 19.3 wt.%, respectively. It should be noted that the initial mercury concentration of the feed stream in all experiments was equal to 1950 micro gr/cm^3. The reported data in Fig. 6 were repeated twice for times 120, 330, and 600 minutes, and the uncertainty was less than 2%. From the sharp variation of the mercury adsorption of MRU-4 against time, it is concluded that its dynamic adsorption is faster than that of Cat-A sorbent. It is supposed that mesopores available in the structure of MRU-4 increase its removal mercury capacity and diffusion coefficient.

Additionally, by comparing structural properties (see Table 2) and mercury adsorption capacities (see Table 3) of the synthesized sorbents, a mesoporous gamma-alumina with an average pore diameter, pore volume, and BET surface area higher than 10 nm, 0.7 cm^3/g, and 260 m^2/g, respectively is suggested for synthesizing a suitable mercury removal sorbent.

Conclusions

In this research, alumina-based sorbents were synthesized to adsorb mercury from the natural gas stream, and their structural and functional specifications were studied. A commercial activated alumina and a synthetic γ-Al_2O_3 were used as supports, and 12 wt% of CuO was impregnated on them to synthesize the mercury removal sorbents. Cat-A and MRU-4 were synthesized using activated alumina and γ-Al_2O_3 supports, respectively. Results confirmed that the sorbent synthesized using the mesoporous γ-Al_2O_3 support performed better than the sorbent synthesized using the microporous activated alumina. After impregnating the active metal, the BET surfaces of those mentioned supports dropped about 14% and 42%, respectively. Consequently, the BET surface area was not a key factor in choosing appropriate support for synthesizing the mercury removal sorbents. After impregnating supports, the micropores were filled by the active metal, and therefore, mesopores were significant in preserving the active surface area of the sorbent. The static adsorption capacities of Cat-A and MRU-4 sorbents were equal to 12.1 and 19.3 wt%, respectively. The mesoporous structure of MRU-4 sorbent enhanced its mercury adsorption capacity, diffusion coefficient, and dynamic adsorption.

Nomenclatures

BET: Brunauer-Emmett-Teller
HPMC: Hydroxypropyl methyl methylcellulose
ID: Internal diameter (mm)
MFC: Mass flow controller
SG: Synthetic gas
XRD: X-ray diffraction
TEM: Transmission electron microscopy
XRF: X-ray fluorescence

References

1. Li, Y., Yu, J., Liu, Y., Huang, R., Wang, Z., & Zhao, Y. (2022). A review on removal of mercury from flue gas utilizing existing air pollutant control devices (APCDs), Journal of Hazardous Materials, 427, 128132, doi.org/10.1016/j.jhazmat.2021.128132.
2. Chalkidisa, A., Jampaiah, D., Hartley, P.G., Sabri, Y.M., & Bhargava S.K. (2020). Mercury in natural gas streams: A review of materials and processes for abatement and remediation, Journal of Hazardous Materials, 382, 1-30., doi.org/10.1016/j.jhazmat.2019.121036.
3. Sun, H., Zhao, S., Ma Y., Wu, J., Liang, P., Yang, D., & Zhang, H. (2018). Effective and regenerable Ag/4A zeolite nanocomposite for Hg0 removal from natural gas, Journal of Alloys and Compounds, 762, 520-527, doi.org/10.1016/j.jallcom.2018.05.222.
4. Zhang, H., Sun, H., Zhang, D., Zhang, W., Chen, S., Li, M., & Liang, P. (2019). Nanoconfinement of Ag nanoparticles inside mesoporous channels of MCM-41 molecule sieve as a regenerable and H_2O resistance sorbent for Hg0 removal in natural gas, Chemical Engineering Journal, 361, 139-147, doi.org/10.1016/j.cej.2018.12.059·
5. Zhang, Z., Wu, J., Li, B., Xu, H., & Liu, D. (2019). Removal of elemental mercury from simulated flue gas by ZSM-5 modified with Mn-Fe mixed oxides, Chemical Engineering Journal, 375, 121946, doi.org/10.1016/j.cej.2019.121946.
6. Rastelli, H., Gorawara, J.K., & Simonetti, D.A. (2017). Process for the removal of mercury from hydrocarbon streams containing oxygen, U.S. Patent No. 9670422.
7. Eckersely, N. (2010). Advanced Mercury Removal Technologies, Hydrocarb. Process, 89(1), 29-35.
8. Ralston, N. (2008). Nano-selenium captures mercury, Nature Nanotechnology, 3, 527–528, doi:10.1038/nnano,.2008.251.
9. Hamzehlouyan, T., Sampara, C., Li, J., Kumar, A., & Epling, W. (2014). Experimental and kinetic study of SO_2 oxidation on a Pt/γ-Al_2O_3 catalyst, Applied Catalysis B: Environmental., 152–153, 108–116, doi.org/10.1016/j.apcatb.2014.01.005.
10. Zhou, Q., Duan, Y-F., Hong, Y-G., Zhu, C., She, M., & Zhang. J. (2015). Experimental and kinetic studies of gas-phase mercury adsorption by raw and bromine modified activated carbon, Fuel Processing Technology, 134, 325–332, doi.org/ 10.1016/j.fuproc.2014.12.052
11. Yang, S., Liu, C., Liu, Z., Yang, B., Xiang, K., & Zhang, C. (2018). High catalytic activity and SO_2-poisoning

resistance of Pd/CuC_{12}/γ-Al_2O_3 catalyst for elemental mercury oxidation, Catalysis Communications, 105, 1–5, doi.org/10.1016/j.catcom.2017.11.001.
12. Zou, S., Liao, Y., Xiong, S., Huang, N., Geng, Y., & Yang, S. (2017). H_2S-modified Fe-Ti spinel: a recyclable magnetic sorbent for recovering gaseous elemental mercury from flue gas as a co-benefit of wet electrostatic precipitators, Environmental Science and Technology, 51(6), 3426–3434, doi.org/ 10.1021/acs.est.6b05765.
13. Liu, W., Vidic, R.D., & Brown, T.D. (2000). Impact of flue gas conditions on mercury uptake by sulfur-impregnated activated carbon, Environmental Science & Technology, 34, 154–159, doi.org/10.1021/es990315i.
14. Li, H., Zhu, L., Wang, J., Li, L., & Shih, K. (2016). Development of nano-sulfide sorbent for efficient removal of elemental mercury from coal combustion fuel gas, Environmental Science & Technology, 50(17), 9551–9557, doi.org/10.1021/acs.est.6b02115.
15. Li, H., Zhu, L., Wang, J., Li, L., Lee, P.H., Feng, Y., & Shih, K. (2017). Effect of nitrogen oxides on elemental mercury removal by nanosized mineral sulfide, Environmental Science & Technology, 51, 8530–8536, doi.org/10.1021/acs.est.7b00224.
16. Liao, Y., Chen, D., Zou, S., Xiong, S., Xiao, X., & Dang, H. (2016). Recyclable naturally derived magnetic pyrrhotite for elemental mercury recovery from flue gas, Environmental Science & Technology, 50(19), 10562–10569, doi.org/10.1021/acs.est.6b03288.
17. Xiang, W., Liu, J., Chang, M., & Zheng, C. (2012) The adsorption mechanism of elemental mercury on CuO (110) surface, Chemical Engineering Journal, 200–202, 91–96, doi.org/ 10.1016/j.cej.2012.06.025.
18. Li, F., Wu, J., Qin, Q., Li, Z., & Huang, X. (2010). Controllable synthesis, optical and photocatalytic properties of CuS nanomaterials with hierarchical structures, Powder Technology, 198, 267–274, doi.org/10.1016/j.powtec.2009.11.018.
19. Liu, W., Xua, H., Liao, Y., Quan, Z., Li, S., Zhao, S., Qu, Z., & Yan, N. (2019). Recyclable CuS sorbent with large mercury adsorption capacity in the presence of SO_2 from non-ferrous metal smelting flue gas, Fuel, 235, 847–854, doi.org/10.1016/j.fuel.2018.08.062.
20. Musmarra, D., Karatza, D., Lancia, A., Prisciandaro, M., & Mazziotti di Celso, G. (2015). A Comparison among Different Sorbents for Mercury Adsorption from Flue Gas, Chemical Engineering Transactions, 43, 2461-2466.
21. Karatza, D., Lancia, A., Musmarra, D., & Zucchini, C. (2000). Study of mercury absorption and desorption on sulfur impregnated carbon, Experimental Thermal and Fluid Science, 21, 150-155 , doi.org/10.1016/S0894-1777(99)00065-5.
22. Leyva-Ramos, R., Medellin-Castillo, N.A., Jacobo-Azuara, A., Mendoza-Barron, J., Landin-Rodriguez, L.E., Martinez-Rosales, J.M., & Aragon-Piña, A. (2008). Fluorine Removal from Water Solution by Adsorption on Activated Adsorption on Activated Alumina Prepared from Pesudo-Boehmite, J. Environ. Eng. Manage., 18, 301-309.
23. Sotomayor, F., Cychosz, K.A., & Thommes, M. (2018). Characterization of Micro/Mesoporous Materials by Physisorption: Concepts and Case Studies, Account of Materials & Surface Research, 3, 34-50.
24. Prins, R. (2020). On the structure of γ-Al_2O_3, Journal of Catalysis, 392, 336-346, doi.org/10.1016/j.jcat.2020.10.010.
25. Soltanali, S., Mashayekhi, M., Seif Mohaddecy S.R. (2020). Comprehensive investigation of the effect of adding phosphorus and/or boron to NiMo/ -Al_2O_3 catalyst in diesel fuel hydrotreating, Process Safety and Environmental Protection, 137, 273–281, doi.org/10.1016/j.psep.2020.02.033.